Global Change Biology
celebrating 20 years

Global Change Biology (2014) **20**, 2886–2902, doi: 10.1111/gcb.12553

Urban expansion dynamics and natural habitat loss in China: a multiscale landscape perspective

CHUNYANG HE[1], ZHIFENG LIU[1,2], JIE TIAN[3] and QUN MA[1,2]

[1]*Center for Human-Environment System Sustainability (CHESS), State Key Laboratory of Earth Surface Processes and Resource Ecology (ESPRE), Beijing Normal University, Beijing 100875, China,* [2]*College of Resources Science & Technology, Beijing Normal University, Beijing 100875, China,* [3]*Department of International Development, Community and Environment, Clark University, Worcester, MA 01610, USA*

Abstract

China's extensive urbanization has resulted in a massive loss of natural habitat, which is threatening the nation's biodiversity and socioeconomic sustainability. A timely and accurate understanding of natural habitat loss caused by urban expansion will allow more informed and effective measures to be taken for the conservation of biodiversity. However, the impact of urban expansion on natural habitats is not well-understood, primarily due to the lack of accurate spatial information regarding urban expansion across China. In this study, we proposed an approach that can be used to accurately summarize the dynamics of urban expansion in China over two recent decades (1992–2012), by integrating data on nighttime light levels, a vegetation index, and land surface temperature. The natural habitat loss during the time period was evaluated at the national, ecoregional, and local scales. The results revealed that China had experienced extremely rapid urban growth from 1992 to 2012 with an average annual growth rate of 8.74%, in contrast with the global average of 3.20%. The massive urban expansion has resulted in significant natural habitat loss in some areas in China. Special attention needs to be paid to the Pearl River Delta, where 25.79% or 1518 km^2 of the natural habitat and 41.99% or 760 km^2 of the local wetlands were lost during 1992–2012. This raises serious concerns about species viability and biodiversity. Effective policies and regulations must be implemented and enforced to sustain regional and national development in the context of rapid urbanization.

Keywords: biodiversity, China, ecoregions, natural habitat loss, nighttime light, urban expansion

Received 6 December 2013; revised version received 29 January 2014 and accepted 11 February 2014

Introduction

The loss of natural habitat is one of the main causes of declines in biodiversity (Pimm & Raven, 2000; Brooks *et al*., 2002; Fahrig, 2003). Many human activities, especially farming and logging, have caused significant natural habitat loss (McKinney, 2002). In addition, rapid urban expansion on a massive scale has also resulted in a substantial loss of natural habitat around the world (McDonald *et al*., 2008; Chao, 2009; Scolozzi & Geneletti, 2012; Seto *et al*., 2012). Specifically, large areas of natural habitat, including forest, grassland, and wetland, have been converted into artificial, impervious (e.g., cement, asphalt) surfaces (McKinney, 2002; Irwin & Bockstael, 2007; Seto *et al*., 2012). Mapping and quantifying natural habitat loss following urban expansion is important for understanding its impact on biodiversity (Grimm *et al*., 2008; McDonald *et al*., 2013; Sushinsky *et al*., 2013).

China has been experiencing remarkable urban expansion since its reform and opening up, primarily due to rapid economic development and population growth (Normile, 2008; Qiu, 2010; Liu *et al*., 2012b). From 1981 to 2011, China's built-up area increased nearly fivefold, from 7.44×10^3 km^2 to 4.36×10^4 km^2 (Ministry of Housing & Urban-Rural Development PRC, 2012). China's widespread urban expansion has resulted in extensive natural habitat loss (Li *et al*., 2006; Xie & Ng, 2013), and has seriously threatened the country's biodiversity (Wang *et al*., 2007; Li *et al*., 2010; McDonald *et al*., 2013). For example, the total area of forest and water coverage decreased from 113.3 km^2 in 1987 to 85.3 km^2 in 1999, with a decline of 24.71% in Wuhan, Hubei, China (Li *et al*., 2006). Similarly, from 1988 to 2008, the Shenzhen River basin experienced a 22% (by 159.48 km^2) decrease (Xie & Ng, 2013). Hence, studying natural habitat loss due to urbanization is particularly crucial in China.

Most studies on urbanization-related habitat loss in China have been conducted at the local (e.g., Li *et al*., 2006) and regional (e.g., Xie & Ng, 2013) scales. Few studies have considered the national scale, due to the lack of a suitable approach for accurately and timely obtaining urban expansion information across the entire country, among other reasons (He *et al*., 2006; Liu *et al*., 2012b).

Correspondence: Dr Chunyang He, tel. +86-10-58804498, fax +86-10-58808460, e-mail: hcy@bnu.edu.cn

Because the integration of multiple sources of remotely sensed data is effective for modeling urban expansion at a large geographic scale (Schneider *et al*., 2003; Lu *et al*., 2008; Cao *et al*., 2009; Tang *et al*., 2012; Yang *et al*., 2013), we quantified and mapped natural habitat loss due to urban expansion in China from 1992 to 2012 by integrating and analyzing three different data sets: data on nighttime light levels, the normalized difference vegetation index (NDVI), and land surface temperature (LST). The spatiotemporal dynamics of urban expansion was modeled at the national, ecoregional, and local levels. Loss was further evaluated in ecoregions and hotspot areas that had experienced significant urban growth.

Materials and methods

Data sources

Nighttime light data. Both the historical time series of nighttime stable light (NSL) data and the newly released NSL data with a better quality (Baugh *et al*., 2013) were collected to cover the time span of our study, including the Version 4 NSL data (1992–2010) collected by the US Air Force Defense Meteorological Satellite Program's Operational Linescan System (DMSP/OLS) and the Visible Infrared Imaging Radiometer Suite (VIIRS) NSL data of 2012 from the Suomi National Polar-orbiting Partnership (NPP) Satellite.

The former was acquired by six DMSP satellites (F10, F12, F14, F15, F16, and F18) and can be obtained from the National Oceanic and Atmospheric Administration's National Geophysical Data Center (NOAA/NGDC) website (http://ngdc.noaa.gov/eog/dmsp/downloadV4composites.html, accessed August 14, 2013). An annual composite image was produced based on images from the year in which all these satellites had the best data quality. The data were also processed to remove the effects of sunlight, glare, moonlight, clouds, and auroras. Ephemeral events such as fires were also discarded (Elvidge *et al*., 2009; Baugh *et al*., 2010). In the annual composites, the digital number (DN) value of each pixel represents the average strength of light from cities, towns, and/or other sites with constant lighting. In each case, the background noise was identified and replaced with a value of 0. The DN values for lit pixels fell in the range of 1–63. The annual NSL composite images produced were subsequently clipped to the administrative boundaries of China. Due to the inherent discontinuity and incomparability of NSL data, the annual composite images were further processed using the approaches introduced by Elvidge *et al*. (2009) and Liu *et al*. (2012b). The processing includes the three key steps of intercalibration, intra-annual composition, and interannual series correction. Please refer to Elvidge *et al*. (2009) and Liu *et al*. (2012b) for more details.

The VIIRS NSL data of 2012 were also obtained from the NOAA/NGDC website (http://ngdc.noaa.gov/eog/viirs/download_viirs_ntl.html, accessed August 14, 2013). These data were delivered as a composite of images taken between April 18–26, 2012 and October 11–23, 2012 (Baugh *et al*., 2013). The VIIRS NSL data were processed in a similar way to the DMSP/OLS NSL data to remove the effects of moonlight and clouds (Baugh *et al*., 2013). The DN values for lit pixels represent the radiance of light at night. The VIIRS NSL data were also clipped to the boundaries of China.

NDVI data. The NDVI data acquired by two different satellites were synthetically used in this study, including NOAA's Advanced Very High Resolution Radiometer (AVHRR) and the French Satellite Pour l'Observation de la Terre's Vegetation Sensor (SPOT/VGT) (Loveland *et al*., 2000; Eva *et al*., 2004). Specifically, a time series of 10-day image composites of the NDVI from NOAA/AVHRR (1992, 1993, 1995, and 1996), and from SPOT/VGT (1998–2012) were downloaded from the United States Geological Survey (USGS) website (http://edc2.usgs.gov/1KM/1kmhomepage.php, accessed August 14, 2013) and from the VITO website (http://free.vgt.vito.be/origin, accessed August 14, 2013), respectively. These data had been radiometrically calibrated, precisely georeferenced, and corrected for atmospheric effects before their distribution. Monthly NDVI image composites were generated by selecting the maximum NDVI value for each pixel from three periods in each month (representing days 1–10, 11–20, and 21 to the end of the month). This maximum value composition (MVC) method served to minimize the effects of cloud cover and the variability of atmospheric optical depth (Holben, 1986). The NDVI composites are believed to be well-suited for the detection of vegetation dynamics at large scales (Loveland *et al*., 2000; Eva *et al*., 2004). Furthermore, based on the works of Lu *et al*. (2008) and Cao *et al*. (2009), we generated an annual MVC image for each year. Although an annual MVC image of NDVI conceals land cover changes within the year, it can effectively reduce contamination by clouds while capturing spatial vegetation characteristics on an annual basis (Lu *et al*., 2008; Cao *et al*., 2009).

LST data. As one of the most commonly used LST data sources (Keramitsoglou *et al*., 2011), the Moderate-resolution Imaging Spectroradiometer (MODIS) 8-day composite imagery of LST from 2000 to 2012 was obtained from the data archive and distribution system of the National Aeronautics and Space Administration (NASA) (http://ladsweb.nascom.nasa.gov, accessed August 14, 2013). Each image is composed of average LST values over an 8-day period (Wan, 2009). Differences in LST between urban and nonurban areas are much more significant at night than during the day (Buyantuyev & Wu, 2009; Zakšek & Oštir, 2012). Therefore, MODIS nighttime LST data would be better suited for distinguishing between urban and nonurban areas (Keramitsoglou *et al*., 2011), and thus this is what we used in the present study. Following Mildrexler *et al*. (2009), we produced an MVC image of LST to capture the nighttime LST characteristics in each year from 2000 to 2012.

All of the NSL, NDVI, and LST images collected for this study were further reprojected to the Albers projection and resampled to a spatial resolution of 1 km.

Land use/cover data. The 1990, 1995, 2000, and 2005 national land use/cover datasets (NLCD) of China were obtained from the Data Sharing Infrastructure of the Earth System Science at the Chinese Academy of Science (http://www.geodata.cn/Portal/index.jsp, accessed August 14, 2013). These datasets were produced at 1 km resolution in the Albers projection through the visual interpretation of Landsat Thematic Mapper (TM) images (Liu *et al*., 2005). The proportion of land use/cover for each pixel was summarized from the original 30 m pixels. These NLCD maps fairly accurately represent actual land-use/cover conditions in China during their corresponding years (Liu *et al*., 2005).

Table 1 Descriptive information of the Landsat TM/ETM+ data used in the study

City covered	Path/row	Date
Beijing	123/32	September 7,1992; May 17, 2012
Nanjing	120/38	October 20, 1992; April 26, 2012
Guangzhou	122/44	November 2, 2012
Kunming	129/43	August 16, 1992; January 20, 2012
Zhengzhou	124/36	October 16, 1992; September 13, 2012
Nanchang	121/40	May 20, 1992; October 10, 2012
Shenyang	119/31	September 10, 2012
Urumqi	143/29	September 2, 2012
	143/30	April 27, 2012

Ecoregional boundaries and species data. The ecoregion boundaries used in our study were obtained from the Terrestrial Ecoregions Database by the World Wide Fund for Nature (WWF) (Olson *et al*., 2001) (http://worldwildlife.org/publications/terrestrial-ecoregions-of-the-world, accessed August 14, 2013). The species information in all of the ecoregions was obtained from the WWF's Wild Finder database (http://worldwildlife.org/publications/wildfinder-database, accessed August 14, 2013). Similar to McDonald *et al*. (2008), for each region of China, we calculated the number of threatened species and classified them into four categories (near threatened, vulnerable, endangered, and critically endangered).

Landsat TM/ETM+ data. Fourteen high-quality Landsat Enhanced Thematic Mapper Plus (ETM+) images were obtained from the Geospatial Data Cloud operated by the Chinese Academy of Sciences (http://www.gscloud.cn, accessed August 14, 2013), to cover the eight mega-cities of China (Beijing, Nanjing, Guangzhou, Kunming, Zhengzhou, Nanchang, Shenyang, and Urumqi) at the start and end of our study period (Table 1).

Socioeconomic census data and administrative boundaries. The 1992, 2000, and 2010 socioeconomic census data, including information on the urban population and gross domestic product (GDP) of each province, were obtained from the Statistical Database of Economic and Social Development by the National Knowledge Infrastructure of China (http://tongji.cnki.net, accessed August 14, 2013). The administrative boundaries for the provinces, cities, and counties were obtained as GIS files from the National Geomatics Center of China.

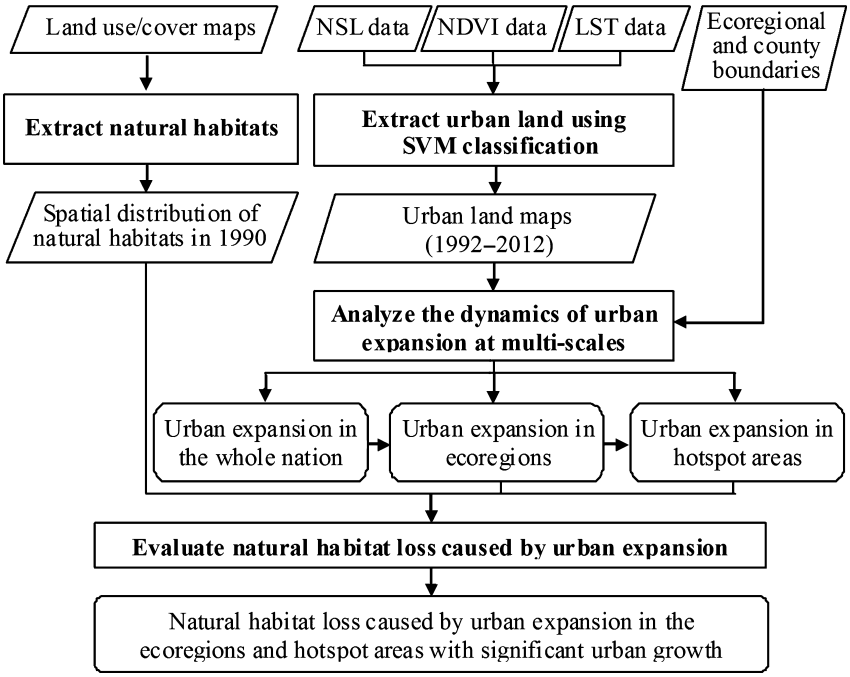

Fig. 1 Methodology flow chart.

Methods

Our method for evaluating natural habitat loss caused by urban expansion included four steps: (i) mapping natural habitats from land use/cover data in 1990; (ii) extracting the area of urban land by applying the support vector machine (SVM) classification method to the NSL, NDVI,and LST data from 1992 to 2012; (iii) analyzing the dynamics of urban expansion at the national, ecoregional, and local scales; and (iv) evaluating natural habitat loss caused by urban expansion in ecoregions and hotspot areas with significant urban growth (Fig. 1).

Mapping natural habitats

The Habitats Classification Scheme developed by the International Union for Conservation of Nature and Natural Resources (IUCN) was adopted in this study (IUCN, 2013), and was used for the extraction of natural habitats from the NLCD of 1990. According to this classification scheme, the term 'natural habitat' refers to any nonartificial vegetation, including forest, grassland, wetlands, and so forth. The more specific land use/cover types in the NLCD were combined into habitat classes (Table 2). Each categorical image of natural habitats was further aggregated from 30 m to 1 km resolution by keeping the percentage area covered by natural habitats for each pixel (Fig. 2).

Extracting urban land

Among the published methods for remotely sensed image classification, the stratified SVM method has been demonstrated as an accurate and reliable one without the need to include any other ancillary data (Cao *et al*., 2009; Yang *et al*., 2013). Therefore, the stratified SVM method (Yang *et al*., 2013) was used with the NSL, NDVI, and LST data to extract urban land areas on a yearly basis, and the urban expansion dynamics were modeled (He *et al*., 2006) for 1992–2012. We used only NSL and NDVI imagery to map urban land in 1992, 1993, 1995, 1996, 1998, and 1999, but also included LST imagery to map urban land through 2000–2010 and 2012.

There is a great variation in physical environment and socio-economic development status across the vast area of China. To mitigate the effects of such variation on urban information extraction, China was divided into eight subregions that are relatively more homogeneous each and distinguishable one from another: northeast, northwest, southwest, northern coastal, southern coastal, eastern coastal, middle reaches of the Yellow River, and middle reaches of the Yangtze River (Development Research Center of the State Council in China, 2005; Yang *et al*., 2013). Training samples of NSL, LST, and NDVI values were taken across the various socioeconomic and physical environments within each subregion (Lu & Weng, 2006; Cao *et al*., 2009; Liu *et al*., 2012b). The SVM classification was subsequently performed with an adaptive post-classification to create a binary map of urban land for China in each year, based on the original NSL, NDVI, and LST images collected.

Table 2 The natural habitat types and their corresponding land use/cover types used in the NLCD

Natural habitat type*	Land use/cover type**	Area (km^2)	Percentage
Forest		2 254 487	29.77%
	Forest	1 373 313	18.13%
	Shrub wood	483 396	6.38%
	Open forest	352 943	4.66%
	Other forest	44 834	0.59%
Grassland		3 038 536	40.12%
	Dense grass	1 004 646	13.27%
	Moderate grass	1 105 256	14.59%
	Sparse grass	928 634	12.26%
Wetlands		288 509	3.81%
	Stream and rivers	36 644	0.48%
	Lakes	75 481	1.00%
	Reservoir and ponds	32 883	0.43%
	Beach and shore	6654	0.09%
	Bottomland	49 549	0.65%
	Swampland	87 297	1.15%
Rocky areas		599 209	7.91%
	Bare rock	599 209	7.91%
Desert		1,094,590	14.45%
	Sandy land	569 896	7.53%
	Gobi	494 775	6.53%
	Bare soil	29 918	0.40%
Other		297 548	3.93%
	Permanent ice and snow	69 670	0.92%
	Salina	135 895	1.79%
	Other unused land	91 983	1.21%
Total		7 572 879	100.00%

*The natural habitat types are standard terms in the Habitats Classification Scheme (Version 3.1) developed by the International Union for Conservation of Nature and Natural Resources (IUCN) (IUCN, 2013).
**The descriptions of land use/cover types in the NLCD can be found in Liu *et al*. (2005).

According to He *et al*. (2006), the urban areas could be assumed to continuously grow outward in China from 1992 to 2012, and an urban pixel with a spatial resolution of 1 km detected by nighttime light data in an earlier year would remain as urban in a later year. Using this assumption, we implemented further data processing with geographical information system (GIS) data to obtain reliable urban dynamics in China (Fig. 3). The data processing can be summarized by the following formula:

$$\mathrm{DN}_{(n,i)} = \begin{cases} 0 & \mathrm{DN}_{(n+1,i)} = 0 \\ 1 & \mathrm{DN}_{(n+1,i)} = 1 \ \& \ \mathrm{DN}_{(n-1,i)} = 1 \\ \mathrm{DN}_{(n,i)} & \text{otherwise} \end{cases} \quad (1)$$

where $\mathrm{DN}_{(n,i)}$, $\mathrm{DN}_{(n-1,i)}$, and $\mathrm{DN}_{(n+1,i)}$ are the class values (urban or non-urban) at the ith pixel in the nth, $n-1$th, and

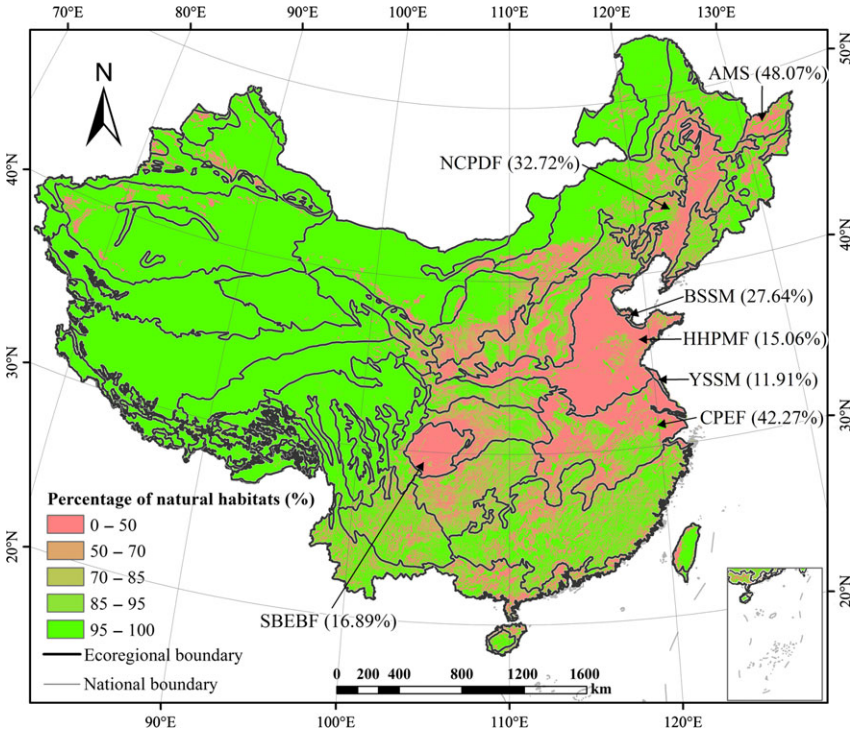

Fig. 2 The spatial distribution of natural habitats in China in 1990 (the ecoregions with a natural habitat loss of less than 50% are labeled using their abbreviations). Yellow Sea saline meadow (YSSM), Huang He Plain mixed forests (HHPMF), Sichuan Basin evergreen broadleaf forests (SBEBF), Bohai Sea saline meadow (BSSM), Northeast China Plain deciduous forests (NCPDE), Changjiang Plain evergreen forests (CPEF), Amur meadow steppe (AMS).

n + 1th years respectively. A class value of 1 represents urban while 0 represents nonurban.

Analyzing the dynamics of urban expansion

Because the spatiotemporal dynamics of urban expansion appear to be significantly different at different scales (Jiang *et al.*, 2012; Wang *et al.*, 2012), we examined it at the national, ecoregional, and local scales.

As an important indicator of urbanization, the growth of the urban area relative to the total area was first calculated for the entire country, each ecoregion, and then each county in China. Ecoregions with a relatively higher growth than the country average were selected for closer examination. At the local scale, spatial autocorrelation analysis (Goodchild, 1986; Anselin, 1995) was performed to identify and map hotspot areas, and clusters of counties with a higher growth in each rapidly urbanizing ecoregion were identified.

Evaluating natural habitat loss caused by urban expansion

According to Hoekstra *et al.* (2004) and Xie & Ng (2013), natural habitat loss caused by urban expansion refers to the conversion of natural habitats into urban land use. Therefore, for evaluation purposes, we calculated the area of each type of natural habitat lost in the urban expansion process for each pixel. The area of habitat type j lost in the i^{th} pixel due to urban expansion was determined using formula 2:

$$\mathrm{HL}_{(i,j)} = \mathrm{HA}_{(i,j)}^{1990} \cdot (\mathrm{Urban}_i^{2012} - \mathrm{Urban}_i^{1992}) \quad (2)$$

where $\mathrm{HL}_{(i,j)}$ is the area of habitat type j lost at the i^{th} pixel from 1992 to 2012; $\mathrm{HA}_{(i,j)}^{1990}$is that for 1990; and Urban_i^{2012} and Urban_i^{1992} are the class values at the i^{th} pixel in the urban land maps in 1992 and 2012 respectively. A class value of 1 represents urban while 0 represents nonurban. The total area of natural habitat loss in each pixel was calculated through summation as shown in formula 3:

$$\mathrm{HL}_i = \sum_{j=1}^{t} \mathrm{HL}_{(i,j)} \quad (3)$$

where HL_i is the total area of natural habitat loss within the i^{th} pixel from 1992 to 2012, and t is the original number of natural habitat types. These calculations were performed for all ecoregions and hotspot areas with significant urban expansion.

Results

Natural habitats of China in 1990

There are a large number of natural habitats, primarily grassland and forest in China (Table 2). In 1990, natural habitats covered 79.26% (7.57 million km^2) of the total

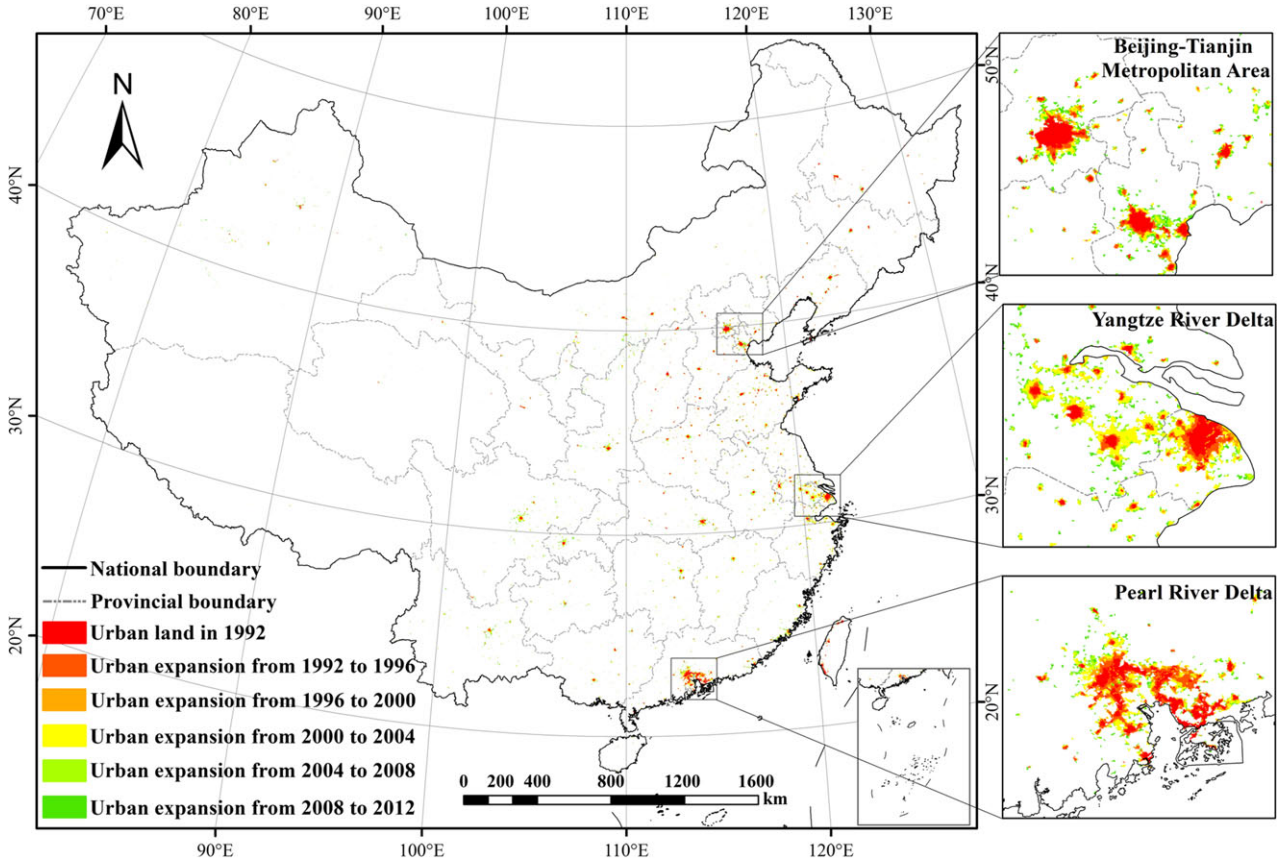

Fig. 3 The dynamics of urban expansion in China from 1992 to 2012.

land area, with grassland and forest accounting for more than 20% of the total land area. Of the total area of natural habitat, grassland and forest made up 40.12% (3.04 million km^2) and 29.77% (2.25 million km^2). All other types accounted for less than 20% each. It should be pointed out that wetland in particular only accounted for 3.81% (0.29 million km^2) of the total natural habitat area.

In terms of spatial distribution, natural habitats are generally more dominant in the west than in the east (Fig. 2), accounting for more than 95% of both the Qinghai-Tibet Plateau (located in southwest China) and the arid and semiarid region of northwest China. However, they generally make up less than 70% of the total area in the monsoon region to the east, and even less than 50% in some subregions (e.g., in all ecoregions of eastern China; Fig. 2). Among these ecoregions, Yellow Sea saline meadow (YSSM), Huang He Plain mixed forest (HHPMF), and Sichuan Basin evergreen broadleaf forests (SBEBF) have particularly low proportions of natural habitat: 11.91% (600.65 km^2), 15.06% (65 112.99 km^2), and 16.89% (16 549.05 km^2) of their total land areas respectively. The Bohai Sea saline meadow (BSSM), Northeast China Plain deciduous forest (NCPDF), Changjiang Plain evergreen forest (CPEF), and Amur meadow steppe (AMS) have relatively higher proportions of natural habitat (20–50%).

Urban expansion in China from 1992 to 2012

China experienced rapid urban expansion over the past two decades, at a much higher rate than the world's average. China's total urban land area increased from 12 192 km^2 (0.13%) in 1992 to 65 186 km^2 (0.68%) in 2012, with an average annual growth rate of 8.74%, while the global average over 1990–2000 was only 3.20% according to Angel *et al.* (2005). Furthermore, the urban expansion rate in China over the past decade far exceeded the annual growth rates of 1.12–4.33% projected by Seto *et al.* (2011) for 2000–2030 under various scenarios.

There was clear spatial disparity in terms of urban expansion when the different ecoregions were compared (Fig. 4). The 16 ecoregions in eastern China experienced a higher rate of urban growth than the national average of 0.55% (Table 3). Among them, the urban

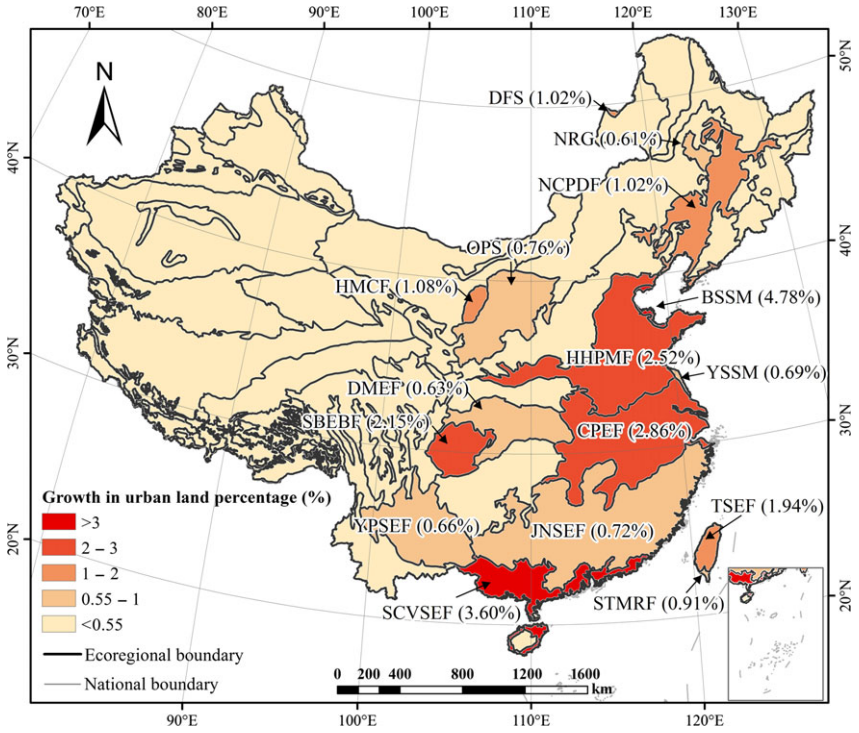

Fig. 4 Urban growth in the ecoregions of China from 1992 to 2012 (ecoregions with a growth rate above the national rate of 0.55% are labeled). Bohai Sea saline meadow (BSSM), South China-Vietnam subtropical evergreen forests (SCVSEF), Changjiang Plain evergreen forests (CPEF), Huang He Plain mixed forests (HHPMF), Sichuan Basin evergreen broadleaf forests (SBEBF), Taiwan subtropical evergreen forests (TSEF), Helanshan montane conifer forests (HMCF), Daurian forest steppe (DFS), Northeast China Plain deciduous forests (NCPDF), South Taiwan monsoon rain forests (STMRF), Ordos Plateau steppe (OPS), Jian Nan subtropical evergreen forests (JNSEF), Yellow Sea saline meadow (YSSM), Yunnan Plateau subtropical evergreen forests (YPSEF), Daba Mountains evergreen forests (DMEF), Nenjiang River grassland (NRG).

area in BSSM increased from 103 km^2 in 1992 to 548 km^2 in 2012, with a net growth of 445 km^2 or 4.78% of the total land area. It is worth noting that around 6580 km^2 of the new urban areas that developed during the time period studied were originally covered by south China–Vietnam subtropical evergreen forests (SCVSEF). In addition, 2–3% of the three ecoregions of CPEF, HHPMF, and SBEBF was urbanized whereas 1–2% of four (e.g., Taiwan subtropical evergreen forest, TSEF) and 0.55–1% of seven (e.g., south Taiwan monsoon rain forest, STMRF) other ecoregions were urbanized (Fig. 4). These 16 ecoregions covering 29.02% of China's land area contained around 85.01% of the newly developed urban areas from 1992 to 2012.

Eight hotspot areas that experienced extremely rapid urban expansion were identified (Fig. 5). In four of them, more than 20% of the land area was converted into urban use from 1992 to 2012. Specifically, these were the Pearl River Delta (32.77%: 4169 km^2), the Yangtze River Delta (27.08%: 5117 km^2), the Changsha-Zhuzhou-Xiangtan area (21.45%: 441 km^2), and the Metropolitan Beijing area (20.83%: 1085 km^2). The three metropolitan areas of Chengdu, Fuzhou-Quanzhou-Xiamen, and Kunming-Yuxi experienced medium levels of urbanization with more than 500 km^2 of newly developed urban area accounting for 10–20% of their total area (Table 4).The Ordos-Yulin area had the lowest percentage (3.54%: 663 km^2) of its land urbanized during the same time period. These eight hotspot areas account for a small fraction (around 0.80%) of China's total land area but contain 27.17% of the country's new urban development in terms of area.

Natural habitat loss at the ecoregional scale

In the 16 ecoregions that experienced significant urban expansion, the rate of natural habitat loss (0.58%) was lower than that of urban growth (1.63%) from 1992 to 2012 (Table 3). However, the area of wetlands decreased by a much higher rate of 3.29%, which is equal to about 3346 km^2 (Fig. 6).

Some ecoregions experienced severe wetland losses such as the alarming 14.07% (923 km^2) decline in

Table 3 The growth in urban land area and the loss of natural habitats caused by significant urban expansion in certain ecoregions

Ecoregion*	Total land area (km^2)	Natural habitats in 1990		Growth in urban land from 1992 to 2012		Natural habitat loss from 1992 to 2012		Richness	Number of threatened species	Endemics	Number of threatened endemic species
		Area (km^2)	Percentage	Area (km^2)	Percentage	Area (km^2)	Percentage				
BSSM	9308	2573	27.64%	445	4.78%	119	4.61%	340	26	0	0
SCVSEF	182 877	112 047	61.27%	6580	3.60%	2103	1.88%	1114	117	62	28
HHPMF	432 457	65 113	15.06%	10 895	2.52%	982	1.51%	618	57	1	0
SBEBF	98 008	16 549	16.89%	2103	2.15%	216	1.31%	630	40	13	10
DFS	2930	2411	82.32%	30	1.02%	25	1.06%	315	22	1	1
CPEF	436 412	184 489	42.27%	12 496	2.86%	1728	0.94%	694	74	11	9
HMCF	24 704	20 715	83.85%	267	1.08%	192	0.93%	258	13	2	2
OPS	215 604	160 947	74.65%	1646	0.76%	1178	0.73%	420	28	2	2
YSSM	5044	601	11.91%	35	0.69%	4	0.65%	319	23	0	0
TSEF	32 877	25 049	76.19%	639	1.94%	119	0.48%	528	48	59	21
NCPDF	230 596	75 454	32.72%	2342	1.02%	338	0.45%	635	57	0	0
NRG	23 260	12 479	53.65%	142	0.61%	53	0.42%	303	25	0	0
STMRF	2 523	1 802	71.45%	23	0.91%	5	0.27%	452	33	36	12
YPSEF	239 854	188 019	78.39%	1590	0.66%	462	0.25%	1038	85	39	19
DMEF	168 170	102 336	60.85%	1062	0.63%	206	0.20%	683	53	13	8
JNSEF	660 811	516 396	78.15%	4757	0.72%	919	0.18%	972	96	44	19
Total	2 765 434	1 486 980	53.77%	45 052	1.63%	8647	0.58%				

*The ecoregion abbreviations are the same as in Fig. 4

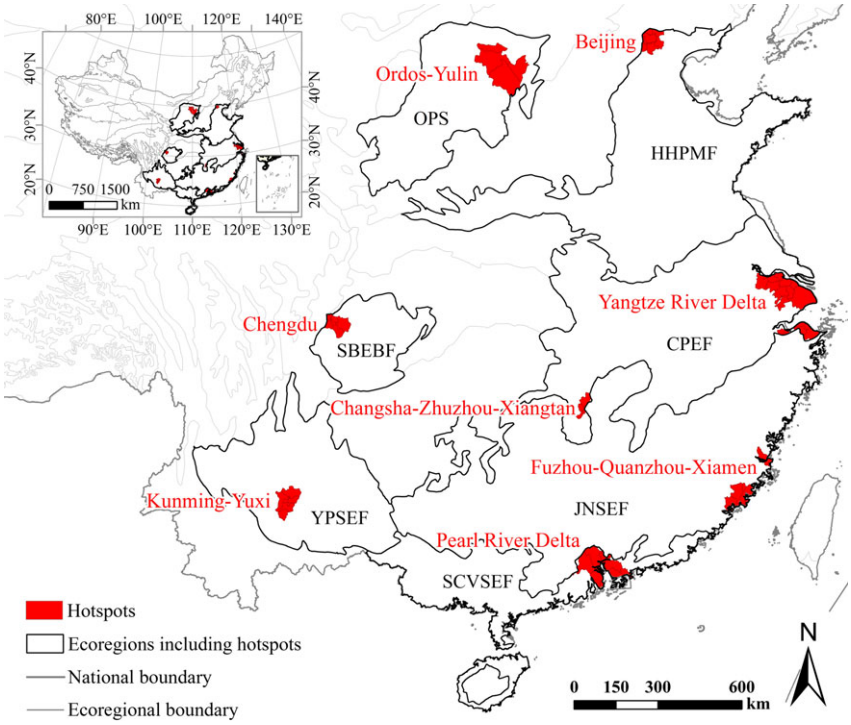

Fig. 5 Hotspot areas with a significant urban expansion from 1992 to 2012. Please refer to Fig. 4 for an explanation of the abbreviations.

Table 4 The growth in urban land area and the loss of natural habitats caused by urban expansion in the hotspot areas

Hotspot	Total land area (km^2)	Natural habitats in 1990		Growth in urban land from 1992 to 2012		Natural habitat loss from 1992 to 2012	
		Area (km^2)	Percentage	Area (km^2)	Percentage	Area (km^2)	Percentage
Pearl River Delta	12 721	5886	46.27%	4169	32.77%	1518	25.79%
Changsha-Zhuzhou-Xiangtan	2056	1017	49.49%	441	21.45%	155	15.25%
Yangtze River Delta	18 895	2740	14.50%	5117	27.08%	356	13.01%
Beijing	5211	601	11.52%	1085	20.82%	63	10.44%
Chengdu	4587	448	9.77%	889	19.38%	29	6.48%
Kunming-Yuxi	6267	4497	71.75%	760	12.13%	250	5.56%
Fuzhou-Quanzhou-Xiamen	7476	3888	52.00%	1276	17.07%	209	5.37%
Ordos-Yulin	18 727	14733	78.67%	663	3.54%	487	3.31%
Total	75 940	33810	44.52%	14 400	18.96%	3068	9.07%

SCVSEF (Fig. 7). Although it was less severe, SBEBF, BSSM, and STMRF also lost a considerable portion (5–10%) of their wetlands during the time period.

Natural habitat loss at the local scale

Widespread urban expansion resulted in a dramatic loss of natural habitat in some hotspot areas during the period of 1992–2012. Around 14 400 km^2 of land surface was converted into urban use from 1992 to 2012 in these areas, which led to a total loss of natural habitat of 3068 km^2 accounting for 9.07% of the total area of natural habitat in 1990 (Table 4).

Specifically, the Pearl River Delta lost 1518 km^2 or 25.79% of its area of natural habitat whereas in the Changsha-Zhuzhou-Xiangtan Metropolitan area, the Yangtze River Delta and the Metropolitan Beijing area loss 10–20% (Table 4). The relatively less urbanized Chengdu, Kunming-Yuxi, and Fuzhou-Quanzhou-Xiamen areas also lost 5–10% of their area of natural habitat.

It should be noted that a highly significant proportion (>30%) of wetlands was lost in the Pearl River

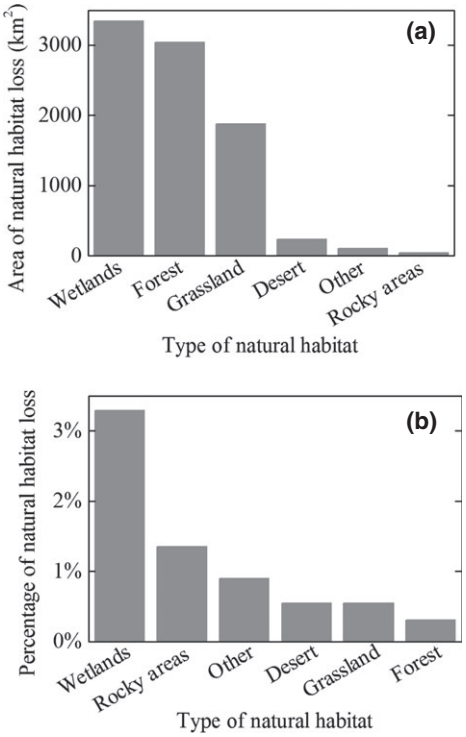

Fig. 6 Overall natural habitat loss by type in ecoregions with significant urban expansion from 1992 to 2012 (a: in area; b: in percentage).

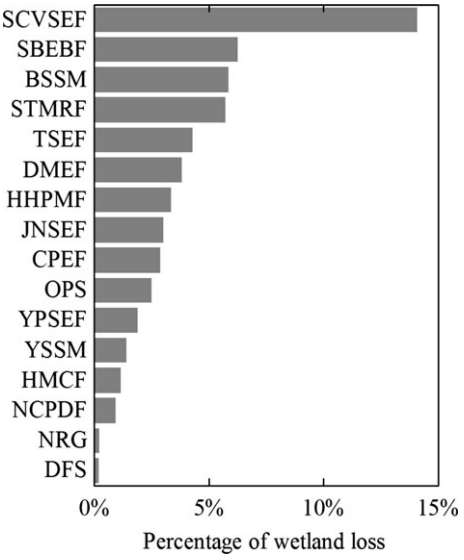

Fig. 7 Wetland loss caused by urban expansion in ecoregions with significant urban expansion from 1992 to 2012. Please refer to Fig. 4 for an explanation of the abbreviations.

Delta, the Changsha-Zhuzhou-Xiangtan area, and the Fuzhou-Quanzhou-Xiamen area (Fig. 8). Special attention should be paid to the Pearl River Delta where an alarming 41.99% or 760 km^2 of wetland was lost.

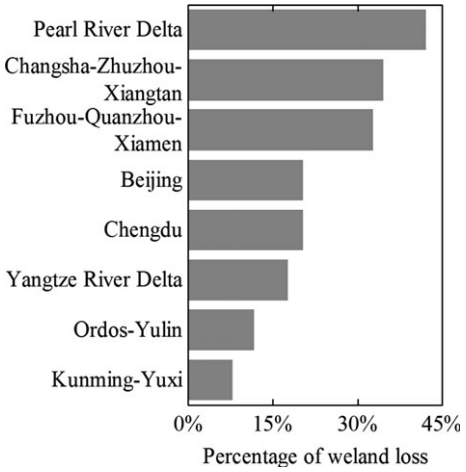

Fig. 8 Wetland loss caused by urban expansion from 1992 to 2012 in the hotspot areas.

Discussion

Integration of NSL, NDVI, and LST data provides a new approach for capturing urban expansion dynamics more timely and accurately at a large scale

Currently, two sources of data are primarily used to model the dynamics of urban expansion in China: socioeconomic census data in administrative units and remotely sensed data at medium to high resolution (e.g., Landsat images). For example, Gu & Pang (2009) and Fang (2009) studied urban expansion before and after the reform and opening up policy was implemented in China, purely based on socioeconomic census data. However, socioeconomic census data do not usually possess the spatial details required for the accurate mapping or analysis of urban expansion. In contrast, Liu *et al.* (2012a) and Wang *et al.* (2012) both used remote-sensing data to study urban expansion dynamics at various spatial scales over the past 20 years in China. One of the major limitations of extracting and mapping urban expansion in this way is that it is computationally intensive and requires a considerable amount of human interpretation. Therefore, timely extraction or mapping is difficult to achieve in such a manner for a vast country such as China.

DMSP/OLS nighttime light data may be an effective alternative data source because its spatial resolution and temporal frequency are suitable for detecting urban expansion at a large scale (Zhang & Seto, 2011). Using DMSP/OLS nighttime light data, He *et al.* (2006) and Liu *et al.* (2012b) modeled urban expansion in China over the periods 1992–1998 and 1992–2008. However, because these light data do not contain spectral

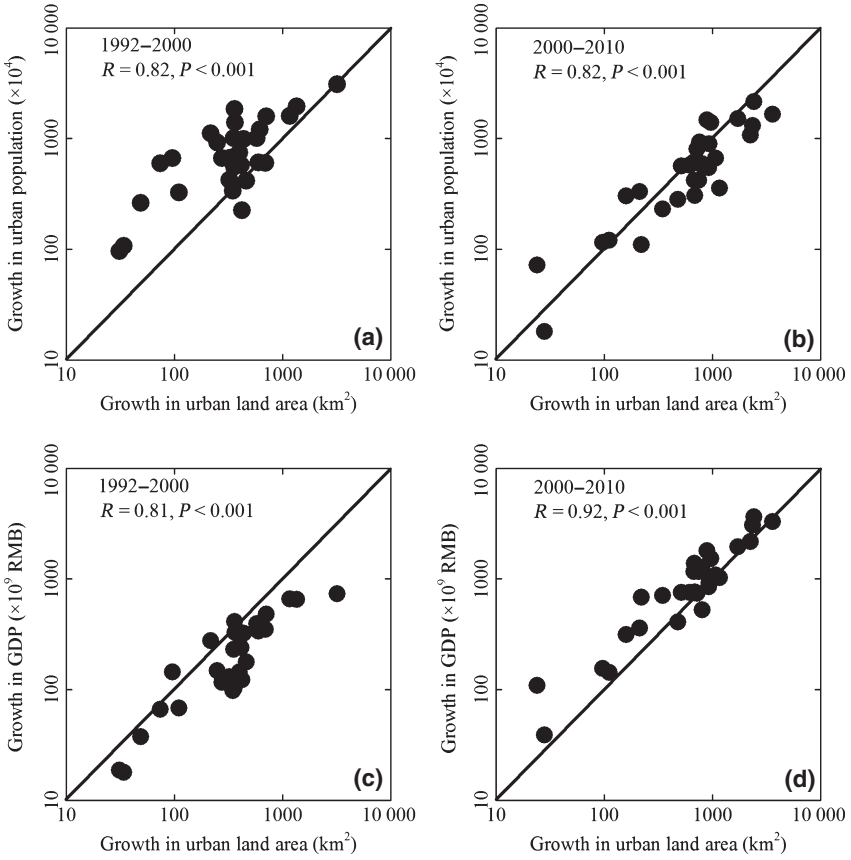

Fig. 9 Correlation between growth in urban land area and growth in urban population and GDP at the province level during 1992–2000 and 2000–2010.

information regarding land cover characteristics, they only indirectly represent the spatial intensity of human activities (Zhang *et al.*, 2013). Furthermore, such data suffer to a degree from overglow and saturation effects (Cao *et al.*, 2009), often leading to less accurate extractions of urban land area (Cao *et al.*, 2009; Zhang *et al.*, 2013).

The integrative approach proposed in this study utilized DMSP/OLS nighttime light data, NDVI data, and LST data and was found to be an effective way for the timely yet accurate mapping of urban expansion in China. The accuracy of our results was assessed in two ways. We first employed an indirect assessment method introduced by Zhang & Seto (2011) and Liu *et al.* (2012b), which relies on socioeconomic census data to evaluate estimated urban expansion at the provincial level. The assessment showed that our estimated results had a strong correlation ($R > 0.8$) with the census data for urban population growth and GDP at a significance level of 0.001 (Fig. 9). In addition, following methods suggested by Sutton *et al.* (2006), Lu *et al.* (2008), and Cao *et al.* (2009), we assessed the spatial accuracy of our estimated urban expansion. In this assessment process, eight important capital cities with various levels of urbanization were selected as sample areas, and the reference urban land uses in these areas were extracted from Landsat TM/ETM+ images and the NLCD. The assessments made for 1995, 2000, 2005, and 2012 resulted in an average Kappa value of 0.66, an average overall accuracy (OA) of 95.20%, an average quantity disagreement (QD) of 2.24%, and an average allocation disagreement (AD) of 2.56% (Figs 10 and 11; Table 5). Moreover, the urban expansion over 1992–2012 was also well-captured (Kappa: 0.58, OA: 92.20%, QD: 2.08% and AD: 5.72%) (Fig. 12). It should be noted that the evaluation results suggest that our method is more accurate in urban information extraction when compared with the method by Cao *et al.* (2009). For instance, the OA with our method reached 93.65% in comparison with the 90.50% in Cao *et al.* (2009), the Kappa improved from 0.62 to 0.70 (Fig. 10; Table 5). The relatively high accuracy suggests that the proposed approach is a fairly efficient and accurate method for monitoring urban expansion dynamics across China.

The reason for the superior performance of our approach is three fold. First, DMSP/OLS nighttime light data can be used to map the intensity of human activities, which is usually highly correlated with the

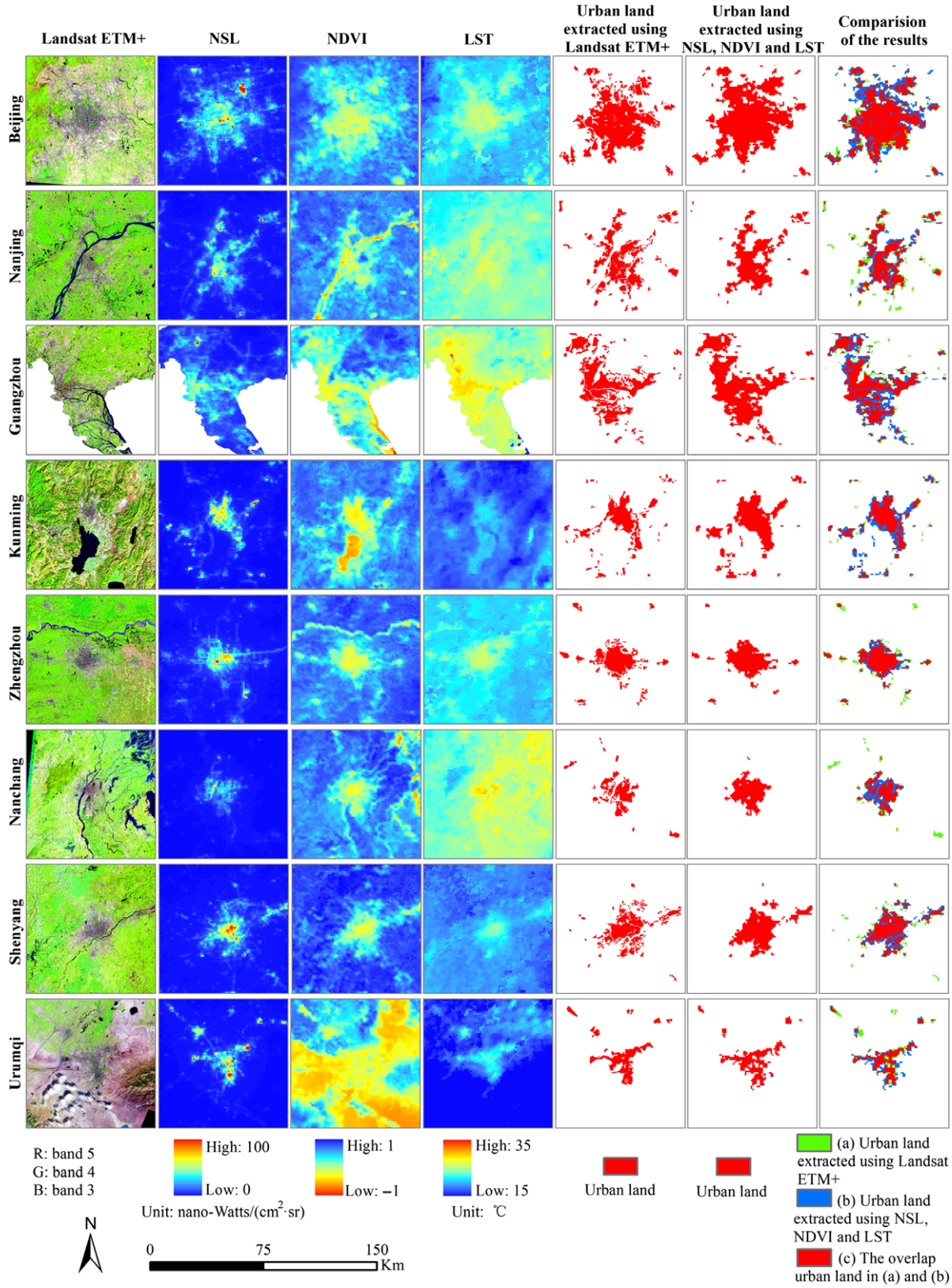

Fig. 10 An assessment of the accuracy of urban land maps generated for selected cities in reference to the classification results of Landsat ETM+ data in 2012.

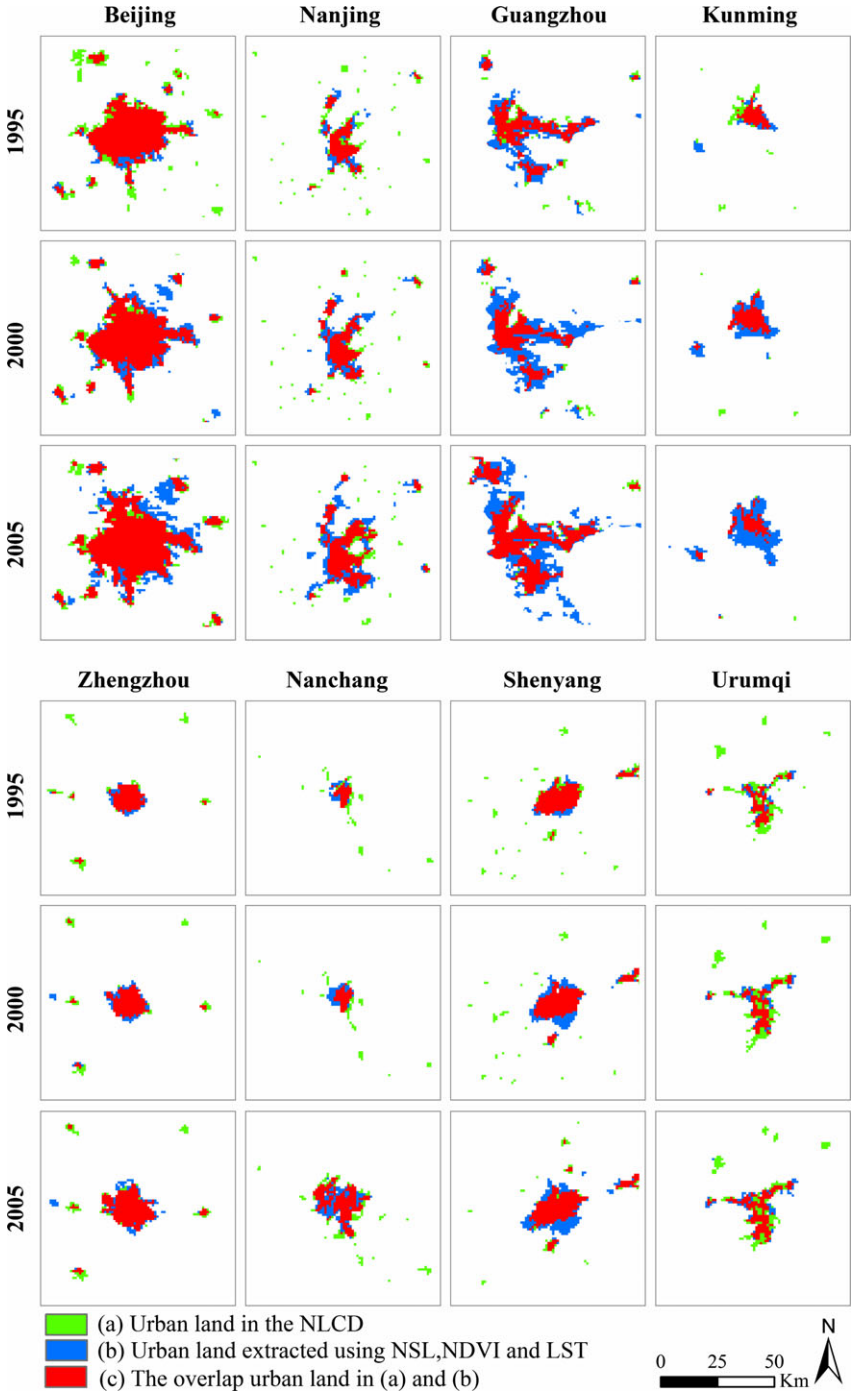

Fig. 11 An assessment of the accuracy of urban land maps generated for selected cities in reference to the NLCD data.

level of urbanization. Second, NDVI data can be effectively used to distinguish between urban areas and nonurban areas that have different vegetation cover characteristics (Zhang *et al.*, 2013). Finally, LST data serve as another layer of information that helps to differentiate urban land surfaces from nonurban surfaces due to their different thermal capacities (Lu & Weng, 2006; Tang *et al.*, 2012).

Moreover, our proposed approach has great potential for use in monitoring or modeling global urban expansion dynamics. Recently, Zhang & Seto (2011) attempted to map urban expansion over the period of 1992–2008 in four urbanized countries including China, the United States, India, and Japan, based on an analysis of DMSP/OLS nighttime light data. The results were relatively inaccurate due to the overglow and

Table 5 An assessment of the accuracy of the urban land maps generated for selected cities in 1995, 2000, 2005, and 2012

Year	Index*	Beijing	Nanjing	Guangzhou	Kunming	Zhengzhou	Nanchang	Shenyang	Urumqi	Average
1995	Kappa	0.77	0.62	0.63	0.61	0.74	0.53	0.76	0.53	0.65
	OA	93.55%	96.37%	93.53%	98.10%	98.31%	98.57%	97.75%	96.96%	96.64%
	QD	3.02%	0.71%	3.58%	0.17%	0.51%	0.51%	0.76%	1.72%	1.37%
	AD	3.43%	2.92%	2.88%	1.73%	1.19%	0.92%	1.49%	1.32%	1.99%
2000	Kappa	0.81	0.66	0.52	0.63	0.75	0.55	0.72	0.55	0.65
	OA	94.11%	95.97%	90.42%	97.21%	98.10%	98.47%	96.93%	96.42%	95.96%
	QD	2.56%	0.80%	8.08%	2.28%	0.07%	0.14%	1.25%	1.82%	2.12%
	AD	3.33%	3.23%	1.49%	0.51%	1.83%	1.39%	1.82%	1.77%	1.92%
2005	Kappa	0.75	0.64	0.64	0.41	0.78	0.69	0.72	0.61	0.65
	OA	90.69%	93.90%	89.96%	94.94%	97.49%	96.80%	96.40%	96.40%	94.57%
	QD	3.92%	2.46%	8.55%	4.93%	0.03%	0.04%	2.10%	1.46%	2.94%
	AD	5.39%	3.64%	1.49%	0.14%	2.48%	3.16%	1.50%	2.14%	2.49%
2012	Kappa	0.71	0.69	0.70	0.69	0.76	0.67	0.72	0.67	0.70
	OA	88.15%	92.94%	90.37%	93.91%	96.27%	96.22%	95.12%	96.21%	93.65%
	QD	6.99%	0.17%	5.47%	4.15%	0.12%	1.28%	1.38%	0.67%	2.53%
	AD	4.87%	6.89%	4.16%	1.94%	3.61%	2.50%	3.50%	3.12%	3.82%
Average	Kappa	0.76	0.65	0.62	0.58	0.76	0.61	0.73	0.59	0.66
	OA	91.63%	94.79%	91.07%	96.04%	97.54%	97.51%	96.55%	96.50%	95.20%
	QD	4.12%	1.04%	6.42%	2.88%	0.18%	0.49%	1.37%	1.42%	2.24%
	AD	4.25%	4.17%	2.51%	1.08%	2.28%	1.99%	2.08%	2.09%	2.56%

*overall accuracy (OA), quantity disagreement (QD) and allocation disagreement (AD).

saturation effects associated with the DMSP/OLS nighttime light data (Zhang & Seto, 2011). Zhang *et al.* (2013) developed a Vegetation Adjusted NTL Urban Index (VANUI) by combining DMSP/OLS nighttime light data values with NDVI data values. Although the use of VANUI was effective for alleviating the confusion between the urban and nonurban areas that had significantly different vegetation cover characteristics, confusion remained between the NDVI values for similar urban and nonurban areas, such as arid or semiarid rural areas vs. suburban areas (Zhang *et al*., 2013). Our proposed approach is expected to improve the accuracy of monitoring/modeling urban expansion in global regions because it utilizes both the social (intensity of human activities) and physical (vegetation cover conditions and surface temperature) indicators of urban development.

Urban expansion has resulted in considerable natural habitat loss, threatening species in various areas of China

During the extremely rapid urban expansion in the last two decades, considerable natural habitat loss had been found primarily in the four identified hotspot areas, including the Pearl River Delta, Changsha-Zhuzhou-Xiangtan, Yangtze River Delta, and the Metropolitan Beijing area, where the area of natural habitat had decreased by more than 10%. The Pearl River Delta is particularly notable for having experienced an alarming 25.79% drop in natural habitat coverage; 42% of the wetlands in this area were converted into other uses.

Loss of habitat is threatening the life and reproduction of many species in many areas (Fig. 13), mainly the four ecoregions of SCVSEF, JNSEF, CPEF, and HHPMF and five hotspot areas (Pearl River Delta, Changsha-Zhuzhou-Xiangtan, Yangtze River Delta, Metropolitan Beijing area, and Fuzhou-Quanzhou-Xiamen). Within these ecoregions, where circa 1000 km^2 or more natural habitats lost, the loss was more pronounced (>75% or 700 km^2) in wetlands and forests, which generally have a higher biodiversity (Fig. 13). As a result of the natural habitat loss, over 600 species have been influenced in each of the four ecoregions (Table 3). At least 50 species of them have been threatened in these areas (Fig. 13; Table 3). Moreover, almost half of the 40+ endemic species in SCVSEF and JNSEF have been threatened (Table 3). Special attention should be paid to SCVSEF, where 117 of the 1114 species and 28 of the 62 endemics species have been confirmed to be threatened by the lasting urban expansion with around 2103 km^2 of natural habitat area lost (Table 3). Continued loss in these already endangered areas will further decrease their biodiversity and disrupt local-regional ecosystems. Therefore, it is very important to better protect the threatened species in these areas and implement effective policies for wildlife conservation in the face of aggressive urban expansion.

Our findings are consistent with results from previous studies (e.g., McDonald *et al*., 2008) in terms of the

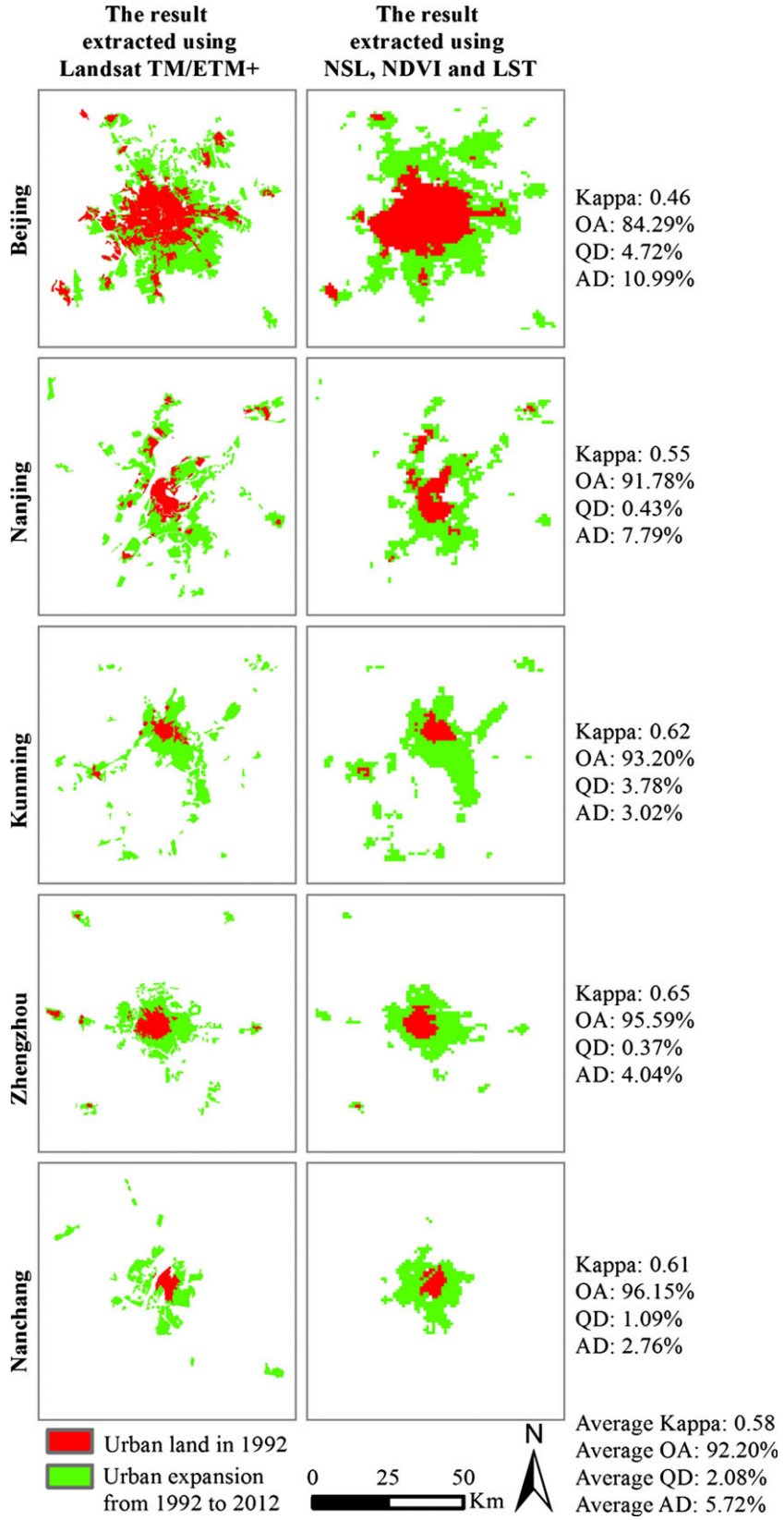

Fig. 12 An assessment of the accuracy of estimated urban expansion from 1992 to 2012 for selected cities in reference to the classification results from the Landsat TM/ETM+ data.

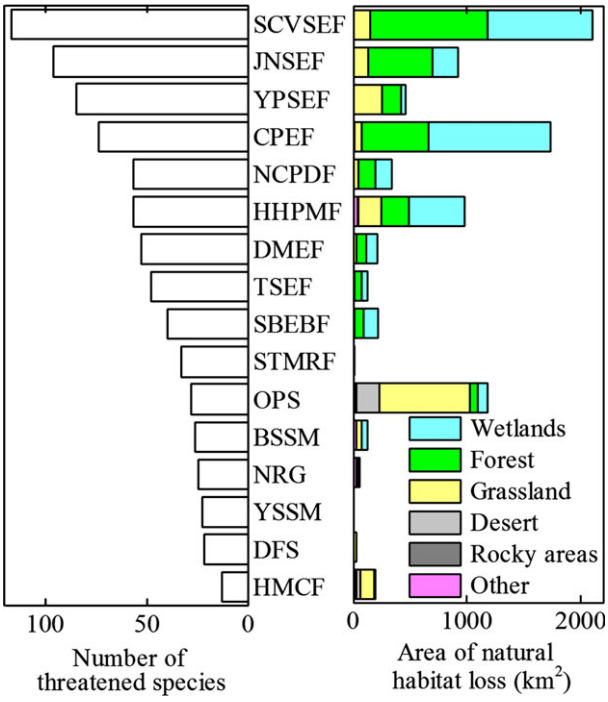

Fig. 13 The number of threatened species and natural habitat loss in the ecoregions with a significant urban expansion from 1992 to 2012. Please refer to Fig. 4 for an explanation of the abbreviations.

imbalance in urban development between eastern and western China, the ecoregions identified (e.g., SCVSEF and HHPMF) as having much higher urban growth rates, and the serious concerns regarding threatened species and decreasing biodiversity.

Limitations and future perspectives

There are a few limitations to our proposed approach. For example, due to the relatively low spatial resolution of the urban land, there were misclassifications, especially in suburban areas (Fig. 10). In addition, natural features such as small water bodies may be classified as urban if they are situated within an urban area, which was the major cause of the relatively lower accuracy in the cities of Guangzhou and Nanchang (Fig. 10).

We investigated the natural habitat loss caused by urban expansion from a geospatial and landscape perspective but the ecological outcomes or mechanisms should also be studied. Moreover, spatial characteristics across different ecosystems within a natural habitat area were not studied, nor was the relationship between landscape patterns and ecological processes.

In future studies, the availability of a VIIRS nighttime light time series dataset with finer spatial resolution is expected to provide a valuable data source for improving the performance of our approach (Elvidge *et al.*, 2007; Zhang *et al.*, 2013). With the increasing spatial resolution of the data, similar studies should be conducted at a local level, so that the impacts of natural habitat loss on ecosystem services can be evaluated using the models offered by software such as the Integrated Valuation of Ecosystem Services and Tradeoffs (InVEST) (Tallis *et al.*, 2013) and Service Path Attribution Networks (SPANs) (Johnson *et al.*, 2012; Bagstad *et al.*, 2013). It will be very informative to apply our approach to monitoring urban expansions in other countries or regions and to make comparisons. An investigation at these three levels is expected to offer a more thorough and comprehensive understanding of the urbanization process in the recent past.

In conclusion, we have proposed a new approach for mapping and monitoring urban expansion through the integrative use of NSL data, NDVI data, and LST data. This approach was shown to be fairly efficient and accurate with an average Kappa value of 0.58 and an average OA of 92.20% when used to estimate urban expansion in China over the period 1992–2012. Natural habitat loss caused by urban expansion was further evaluated at multiple scales. The results clearly showed that urban expansion in China has resulted in severe natural habitat loss in some areas. Special attention needs to be paid to the Pearl River Delta, where 25.79% (1518 km^2) of natural habitat including 41.99% (760 $km^{2)}$ of the wetlands were lost during 1992–2012. This raises serious concerns about species viability and biodiversity. Effective policies and regulations must be implemented and enforced to sustain regional and national development in the context of rapid urbanization.

Acknowledgements

We would like to thank Prof. Jianguo Wu from Arizona State University, USA for his helpful suggestions on the initiative idea of the article. We also want to express our respects and gratitude to the anonymous reviewers and editors for their valuable comments on improving the quality of the paper. Our research has been supported in part by the National Natural Science Foundation of China (Grant No. 41222003 & No. 41311001) and the National Basic Research Programs of China (Grant No. 2014CB954302&2010CB950901). It was also supported by the 111 project 'Hazard and Risk Science Base at Beijing Normal University' under Grant B08008, China.

References

Angel S, Sheppard SC, Civco DL (2005) *The Dynamics of Global Urban Expansion*. Washington D.C, The World Bank.

Anselin L (1995) Local Indicators of Spatial Association–LISA. *Geographical Analysis*, **27**, 93–115.

Bagstad KJ, Johnson GW, Voigt B, Villa F (2013) Spatial dynamics of ecosystem service flows: a comprehensive approach to quantifying actual services. *Ecosystem Services*, **4**, 117–125.

Baugh KE, Elvidge CD, Ghosh T, Ziskin D (2010) Development of a 2009 stable lights product using DMSP-OLS data. *Proceedings of the Asia-Pacific Advanced Network*, **30**, 114–130.

Baugh KE, Hsu FC, Elvidge CD, Zhizhin M (2013) Nighttime lights compositing using the VIIRS day-night band: preliminary results. *Proceedings of the Asia-Pacific Advanced Network 2013*, **35**, 70–86.

Brooks TM, Mittermeier RA, Mittermeier CG *et al*. (2002) Habitat loss and extinction in the hotspots of biodiversity. *Conservation Biology*, **16**, 909–923.

Buyantuyev A, Wu J (2009) Urban heat islands and landscape heterogeneity: linking spatiotemporal variation in surface temperatures to land-cover and socioeconomic patterns. *Landscape Ecology*, **25**, 17–33.

Cao X, Chen J, Imura H, Higashi O (2009) A SVM-based method to extract urban areas from DMSP-OLS and SPOT VGT data. *Remote Sensing of Environment*, **113**, 2205–2209.

Chao R (2009) Effects of increased urbanization. *Science*, **324**, 37–37.

Development Research Center of the State Council in China (2005) Coordinated regional development strategy and policy reports. Available at: http://www.cqvip.com/QK/85199X/200565/15595896.html

Elvidge CD, Cinzano P, Pettit DR *et al*. (2007) The Nightsat mission concept. *International Journal of Remote Sensing*, **28**, 2645–2670.

Elvidge CD, Ziskin D, Baugh KE *et al*. (2009) A fifteen year record of global natural gas flaring derived from satellite data. *Energies*, **2**, 595–622.

Eva HD, Belward AS, De Miranda EE *et al*. (2004) A land cover map of South America. *Global Change Biology*, **10**, 731–744.

Fahrig L (2003) Effects of habitat fragmentation on biodiversity. *Annual Review of Ecology Evolution and Systematics*, **34**, 487–515.

Fang C (2009) Urbanization and urban development in China after the reform and opening-up. *Economic Geography*, **29**, 19–25.

Goodchild MF (1986) *Spatial Autocorrelation*. Geo Books, Norwich.

Grimm NB, Faeth SH, Golubiewski NE, Redman CL, Wu J, Bai X, Briggs JM (2008) Global change and the ecology of cities. *Science*, **319**, 756–760.

Gu C, Pang H (2009) Evolution of Chinese urbanization spaces: kernel spatial approach. *Scientia Geographical Sinica*, **29**, 10–14.

He C, Shi P, Li J *et al*. (2006) Restoring urbanization process in China in the 1990s using non-radiance-calibrated DMSP/OLS nighttime light imagery and statistical data. *Chinese Science Bulletin*, **51**, 1614–1620.

Hoekstra JM, Boucher TM, Ricketts TH, Roberts C (2004) Confronting a biome crisis: global disparities of habitat loss and protection. *Ecology Letters*, **8**, 23–29.

Holben BN (1986) Characteristics of maximum-value composite images from temporal AVHRR data. *International Journal of Remote Sensing*, **7**, 1417–1434.

Irwin EG, Bockstael NE (2007) The evolution of urban sprawl: evidence of spatial heterogeneity and increasing land fragmentation. *Proceedings of the National Academy of Sciences of the United States of America*, **104**, 20672–20677.

IUCN (2013) Habitats classification scheme (Version 3.1). In: *The IUCN Red List of Threatened Species (Version 2013.1)*. Available at: http://www.iucnredlist.org.

Jiang L, Deng XZ, Seto KC (2012) Multi-level modeling of urban expansion and cultivated land conversion for urban hotspot counties in China. *Landscape and Urban Planning*, **108**, 131–139.

Johnson GW, Bagstad KJ, Snapp RR, Villa F (2012) Service patch attribution networks (SPANs): a network flow approach to ecosystem service assessment. *International Journal of Agricultural and Environmental Information Systems*, **3**, 54–71.

Keramitsoglou I, Kiranoudis CT, Ceriola G, Weng Q, Rajasekar U (2011) Identification and analysis of urban surface temperature patterns in Greater Athens, Greece, using MODIS imagery. *Remote Sensing of Environment*, **115**, 3080–3090.

Li Y, Zhao S, Zhao K, Xie P, Fang J (2006) Land-cover changes in an urban lake watershed in a mega-city, Central China. *Environmental Monitoring and Assessment*, **115**, 349–359.

Li T, Shilling F, Thorne J, Li F, Schott H, Boynton R, Berry AM (2010) Fragmentation of China's landscape by roads and urban areas. *Landscape Ecology*, **25**, 839–853.

Liu J, Liu M, Tian H *et al*. (2005) Spatial and temporal patterns of China's cropland during 1990–2000: an analysis based on Landsat TM data. *Remote Sensing of Environment*, **98**, 442–456.

Liu J, Zhang Q, Hu Y (2012a) Regional differences of China's urban expansion from late 20th to early 21st century based on remote sensing information. *Chinese Geographical Science*, **22**, 1–14.

Liu Z, He C, Zhang Q, Huang Q, Yang Y (2012b) Extracting the dynamics of urban expansion in China using DMSP-OLS nighttime light data from 1992 to 2008. *Landscape and Urban Planning*, **106**, 62–72.

Loveland TR, Reed BC, Brown JF, Ohlen DO, Zhu Z, Yang L, Merchant JW (2000) Development of a global land cover characteristics database and IGBP DISCover from 1 km AVHRR data. *International Journal of Remote Sensing*, **21**, 1303–1330.

Lu D, Weng Q (2006) Use of impervious surface in urban land-use classification. *Remote Sensing of Environment*, **102**, 146–160.

Lu D, Tian H, Zhou G, Ge H (2008) Regional mapping of human settlements in southeastern China with multisensor remotely sensed data. *Remote Sensing of Environment*, **112**, 3668–3679.

McDonald RI, Kareiva P, Forman RTT (2008) The implications of current and future urbanization for global protected areas and biodiversity conservation. *Biological Conservation*, **141**, 1695–1703.

McDonald RI, Marcotullio PJ, Güneralp B (2013) Urbanization and global trends in biodiversity and ecosystem services. In: *Urbanization, Biodiversity and Ecosystem Services: Challenges and Opportunities*. (eds Elmqvist T, Fragkias M, Goodness J, Güneralp B, Marcotullio PJ, Mcdonald RI, Parnell S, Schewenius M, Sendstad M, Seto KC, Wilkinson C), pp. 31–52. Springer, the Netherlands.

McKinney ML (2002) Urbanization, biodiversity, and conservation. *BioScience*, **52**, 883–890.

Mildrexler DJ, Zhao M, Running SW (2009) Testing a MODIS global disturbance index across North America. *Remote Sensing of Environment*, **113**, 2103–2117.

Ministry of Housing and Urban-Rural Development PRC (2012) *China Urban Construction Statisitcal Yearbook 2011*. China Planning Press, Beijing.

Normile D (2008) China's living laboratory in urbanization. *Science*, **319**, 740–743.

Olson DM, Dinerstein E, Wikramanayake ED *et al*. (2001) Terrestrial ecoregions of the worlds: a new map of life on Earth. *BioScience*, **51**, 933–938.

Pimm SL, Raven P (2000) Biodiversity-extinction by numbers. *Nature*, **403**, 843–845.

Qiu J (2010) Q&A: Peter Hessler on urbanization in China. *Nature*, **464**, 166–166.

Schneider A, Friedl MA, Mclver DK, Woodcock CE (2003) Mapping urban areas by fusing multiple sources of coarse resolution remotely sensed data. *Photogrammetric Engineering & Remote Sensing*, **69**, 1377–1386.

Scolozzi R, Geneletti D (2012) A multi-scale qualitative approach to assess the impact of urbanization on natural habitats and their connectivity. *Environmental Impact Assessment Review*, **36**, 9–22.

Seto KC, Fragkias M, Güneralp B, Reilly MK (2011) A meta-analysis of global urban land expansion. *PLoS ONE*, **6**, e23777.

Seto KC, Guneralp B, Hutyra LR (2012) Global forecasts of urban expansion to 2030 and direct impacts on biodiversity and carbon pools. *Proceedings of the National Academy of Sciences of the United States of America*, **109**, 16083–16088.

Sushinsky JR, Rhodes JR, Possingham HP, Gill TK, Fuller RA (2013) How should we grow cities to minimize their biodiversity impacts? *Global Change Biology*, **19**, 401–410.

Sutton PC, Cova TJ, Elvidge CD (2006) Mapping 'Exurbia' in the conterminous United States using nighttime satellite imagery. *Geocarto International*, **21**, 39–45.

Tallis HT, Ricketts T, Guerry AD *et al*. (2013) *InVEST 2.5.6 User's Guide*. Stanford, The Natural Capital Project. Available at: http://ncp-dev.stanford.edu/~dataportal/invest-releases/documentation/2_5_6/

Tang Q, Wang L, Li B, Yu JY (2012) Towards a comprehensive evaluation of V-I-S sub-pixel fractions and land surface temperature for urban land-use classification in the USA. *International Journal of Remote Sensing*, **33**, 5996–6019.

Wan Z (2009) *Collection-5 MODIS Land Surface Temperature Products Users' Guide*. University of California, Santa Barbara.

Wang G, Jiang G, Zhou Y *et al*. (2007) Biodiversity conservation in a fast-growing metropolitan area in China: a case study of plant diversity in Beijing. *Biodiversity and Conservation*, **16**, 4025–4038.

Wang L, Li C, Ying Q *et al*. (2012) China's urban expansion from 1990 to 2010 determined with satellite remote sensing. *Chinese Science Bulletin*, **57**, 2802–2812.

Xie YJ, Ng CN (2013) Exploring spatiotemporal variation in habitat loss and its causal factors in the Shenzhen River cross-border watershed. *Applied Geography*, **39**, 140–150.

Yang Y, He CY, Zhang QF, Han LJ, Du SQ (2013) Timely and accurate national-scale mapping of urban land in China using Defense Meteorological Satellite Program's Operational Linescan System nighttime stable light data. *Journal of Applied Remote Sensing*, **7**, 073535.

Zakšek K, Oštir K (2012) Downscaling land surface temperature for urban heat island diurnal cycle analysis. *Remote Sensing of Environment*, **117**, 114–124.

Zhang Q, Seto KC (2011) Mapping urbanization dynamics at regional and global scales using multi-temporal DMSP/OLS nighttime light data. *Remote Sensing of Environment*, **115**, 2320–2329.

Zhang Q, Schaaf C, Seto KC (2013) The vegetation adjusted NTL urban index: a new approach to reduce saturation and increase variation in nighttime luminosity. *Remote Sensing of Environment*, **129**, 32–41.